

# Off-axis short GRBs from structured jets as counterparts to GW events

Adithan Kathirgamaraju<sup>1\*</sup>, Rodolfo Barniol Duran<sup>2\*</sup>, Dimitrios Giannios<sup>1\*</sup>

<sup>1</sup>*Department of Physics and Astronomy, Purdue University, 525 Northwestern Avenue, West Lafayette, IN 47907, USA*

<sup>2</sup>*Department of Physics and Astronomy, California State University, Sacramento, 6000 J Street, Sacramento, CA 95819, USA*

Accepted to MNRAS Letters

## ABSTRACT

Binary neutron star mergers are considered to be the most favorable sources that produce electromagnetic (EM) signals associated with gravitational waves (GWs). These mergers are the likely progenitors of short duration gamma-ray bursts (GRBs). The brief gamma-ray emission (the “prompt” GRB emission) is produced by ultra-relativistic jets, as a result, this emission is strongly beamed over a small solid angle along the jet. It is estimated to be a decade or more before a short GRB jet within the LIGO volume points along our line of sight. For this reason, the study of the prompt signal as an EM counterpart to GW events has been sparse. We argue that for a realistic jet model, one whose luminosity and Lorentz factor vary smoothly with angle, the prompt signal can be detected for a significantly broader range of viewing angles. This can lead to an “off-axis” short GRB as an EM counterpart. Our estimates and simulations show that it is feasible to detect these signals with the aid of the temporal coincidence from a LIGO trigger, even if the observer is substantially misaligned with respect to the jet.

**Key words:** gravitational waves – gamma-ray burst: general – methods: numerical

## 1 INTRODUCTION

The monumental discovery of gravitational waves by the LIGO collaboration enables us to observe our Universe at a new wavelength (Abbott et al. 2016a,c). In particular, gravitational waves allow us to study the merger of compact objects and their properties, offering exquisite tests of general relativity (Abbott et al. 2016d). The next related major quest in astronomy is the discovery of an electromagnetic signal produced during such a merger that accompanies the gravitational waves. We will refer to this specific electromagnetic signal as an electromagnetic “counterpart.”

By far the most promising source of gravitational waves (GWs) and accompanying electromagnetic (EM) signals are double neutron star (NS-NS) mergers (or neutron star-black hole mergers), hereafter referred to as simply “mergers” (e.g., Lee & Ramirez-Ruiz 2007). Such mergers make for promising detectable GW sources by LIGO within a few hundreds of Mpc (Martynov et al. 2016). There are several lines of indirect evidence that suggests these mergers are the most likely progenitors of short GRBs (Eichler et al. 1989; Nakar 2007; Berger 2014). However, a simultaneous GW and GRB detection would provide a most conclusive evidence that short GRBs are indeed produced during binary mergers.

The “prompt”  $\gamma$ -ray emission from short GRBs is believed to be strongly beamed along an ultra-relativistic jet with half opening angle  $\theta_j$  and Lorentz factor  $\Gamma_{\text{core}} \gtrsim 30$  (e.g., Nakar 2007). If

$\Gamma_{\text{core}}\theta_j > 1$ , it will be extremely difficult to detect the prompt emission from a short GRB jet that is misaligned by an angle  $\theta > \theta_j$  with respect to Earth. In fact, the observed rate of short GRBs indicates that it will be a decade or more before the luminous core of a GRB is detected within the LIGO detectability volume of neutron star mergers (e.g., Wanderman & Piran 2015). This has tended to steer investigations of EM counterparts away from the prompt emission (see however Kochanek & Piran 1993; Patricelli et al. 2016; Lazzati et al. 2017), and more towards the less prompt signals that follow days to months after the merger/GW detection; such as “macronova” or “kilonova”, off-axis afterglows and radio flares (e.g., Li & Paczyński 1998; Metzger et al. 2010; Metzger & Berger 2012; Kasen, Badnell & Barnes 2013; Nakar & Piran 2011; Hotokezaka & Piran 2015; Lamb & Kobayashi 2017). Given the poor localization of LIGO (Abbott et al. 2016b), the faintness of these signals, and their long delay, such detections and their association to the merger will be challenging (e.g., Metzger & Berger 2012).

Here we investigate a different, prompt signal from the merger; that of the prompt emission from the moderately relativistic  $\Gamma \sim$  a few part of the jet, the “sheath”, that beams its emission towards the observer (who is located at a substantial angle with respect to the jet’s core). In this letter, we argue that by exploiting the timing from a LIGO trigger, one can reliably detect the prompt emission even if the jet is significantly misaligned with respect to Earth. This is because, in any realistic jet model, there is expected to be a slower, under-luminous sheath surrounding the bright jet core (e.g., Rossi, Lazzati & Rees 2002; Salafia et al. 2015). To quantify this claim, we perform large-scale relativistic magneto-

\* Email: akathirg@purdue.edu (AK), barniolduran@csus.edu (RBD), dgiannio@purdue.edu (DG)

hydrodynamical (MHD) simulations, which follow the jet from the launching region, through the confining ambient gas and the breakout distance where its slower sheath forms. We also provide a calculation to estimate the observed luminosity for an observer located at an arbitrary angle with respect to the jet axis. We find that this endeavor is quite promising.

## 2 OUR MODEL: A STRUCTURED JET

Just prior to the merger of a binary neutron star system, gravitational and hydrodynamical interactions expel some neutron star material, forming the “dynamical ejecta” (e.g., Hotokezaka et al. 2013; Rosswog 2013). The neutron star merger may be followed by the launching of an ultra-relativistic jet. As investigated by previous hydro simulations, the jet is initially collimated by the dynamical ejecta until it breaks out from the surrounding gas (Nagakura et al. 2014; Murguia-Berthier et al. 2014; Duffell, Quataert & MacFadyen 2015). At a larger distance, it dissipates its energy, resulting in a short GRB which lasts for  $\lesssim 2$  s and peaks at  $\sim$  MeV energies (Nakar 2007; Berger 2014). In the majority of previous models, this jet consists of a core having uniform luminosity ( $L_{\text{core}}$ ) and Lorentz factor ( $\Gamma_{\text{core}}$ ) that discontinuously disappears for angles  $\theta > \theta_j$ . However, these models are not physical and greatly underestimate the prompt emission that may be received by observers who are not aligned within the core of the jet (i.e., off-axis observers).

Recent numerical (e.g., Tchekhovskoy, Narayan & McKinney 2010; Komissarov, Vlahakis & Königl 2010) and theoretical (e.g., Sapountzis & Vlahakis 2014) studies show that once a magnetized jet breaks out of the collimating medium, it is expected to develop some “lateral structure”. This means that the jet’s luminosity and Lorentz factor depend on the polar angle  $\theta$  (see Fig. 1). We find that this extended lateral part, though slower and less luminous, can contribute a significant amount of prompt emission for angles larger than  $\theta_j$ . As a result, it is possible to detect the prompt emission from a structured jet for observing angles ( $\theta_{\text{obs}}$ ) much larger than  $\theta_j$ . We call this prompt emission detected by observers with  $\theta_{\text{obs}} > \theta_j$  an “off-axis” short GRB, this is not off-axis as defined in the traditional sense because our jet does not abruptly vanish at  $\theta_j$ . Below we provide an estimate for the prospects and feasibility of detecting this “off-axis” prompt emission and mention some of its advantages over other EM counterparts.

### 2.1 Feasibility of detecting the prompt emission from a structured jet

There are currently more than thirty short GRBs with measured redshift (Fong et al. 2015), and their average redshift is  $\sim 0.5$  (Berger 2014). Let us now pick a typical short GRB with known redshift, assume it takes place within the LIGO detectability volume, and estimate its off-axis prompt emission. Had short GRB101219A (see table 1) taken place at a distance of  $\sim 200$  Mpc, it would have resulted in an extremely bright source with a count rate of  $\sim 10^6$  photons/s at the *Fermi*/GBM detector. This is a factor of  $f \sim 10^4$  above the count rate required for a robust detection of a source coincident with a LIGO trigger by *Fermi* (Connaughton et al. 2016). With such a large on-axis count rate, even a steeply declining luminosity for the lateral structure of the jet will provide a significant amount of off-axis emission that can be detectable by, e.g., *Fermi*. Assuming, for the sake of an estimate, a jet with a core of luminosity  $L_{\text{core}}$  and half opening angle  $\theta_j$ , we can

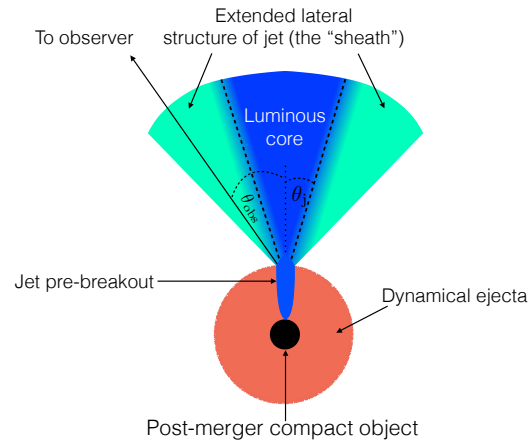


**Figure 1.** A schematic of a short GRB jet. Mergers produce GWs detectable by LIGO and are the likely progenitors of short GRBs. The prompt emission from the jet’s luminous core (routinely observed as a short GRB) is strongly beamed and can only be detected by observers located within  $\theta_j$  from the jet axis. However, the jet is expected to have a lateral structure that moves slower and is fainter than the luminous core. Given the proximity of a LIGO-triggered short GRB, *Fermi* and *Swift* can potentially detect the prompt emission from this lateral structure even if the jet is misaligned with respect to our line of sight (see Section 2.1).

take the luminosity for angles  $\theta > \theta_j$  (i.e. for the lateral structure of the jet) to drop sharply as  $L_{\text{obs}}(\theta) = L_{\text{core}}(\theta/\theta_j)^{-6}$  (Pescalli et al. 2015). Such a jet can still be detected by an observer up to an angle  $\theta_{\text{obs}} \sim f^{1/6}\theta_j \sim 5\theta_j$ . This makes it  $(\theta_{\text{obs}}/\theta_j)^2 \sim 20$  times more likely to observe the sheath of the jet in comparison to its core emission. Instead of detecting about 1 EM counterpart per decade from the prompt core emission, the sheath potentially results in  $\sim$ a few events per year for an instrument with *Fermi*’s field of view, increasing the chances to detect such events tremendously. Therefore, the prompt emission from a short GRB could be detected even if the jet is significantly misaligned.

It is quite likely that the off-axis  $\gamma$ -ray emission, by itself, is not sufficiently bright enough to result in a detector trigger. Nevertheless, using the timing of a LIGO trigger can make even a faint  $\gamma$ -ray signal a statistically significant detection. A faint  $\gamma$ -ray signal must come within several seconds after a LIGO trigger to make such a detection possible (Connaughton et al. 2016). Here, we estimate the temporal difference of these signals. The GW signal, as detected by LIGO, is expected to peak approximately when the merger takes place. The merger will probably initially give birth to a fast-rotating, massive proto-neutron star and can take  $\sim$  hundred milliseconds to collapse to a black hole (e.g., Rezzolla et al. 2011). It is likely that the jet forms a few dynamical times later or, all in all,  $\sim 0.1 - 1$  sec after the GW signal peak, then the jet has to breakout of the collimating medium which can take a few hundreds of msec (Nagakura et al. 2014), and expand to a radius  $r_{\text{jet}}$ , where it radiates. The emission from the jet will, therefore, be further delayed by  $r_{\text{jet}}/\Gamma^2 c$ , where  $\Gamma$  is the Lorentz factor of the patch of the jet directed towards the observer. The fast rise and variability of short GRBs indicates the jet core is characterized by  $r_{\text{jet}}/\Gamma_{\text{core}}^2 c \sim 10$  msec. In Section 4, we argue that the sheath emission is also likely characterized by a delay of  $r_{\text{jet}}/\Gamma^2 c \sim$ a few seconds, i.e., making a very prompt signal.

The misaligned or “off-axis” prompt emission of short GRBs has largely been ignored. The community has rather focused

GRB	$T_{90}$	Fluence	$\beta$	$z$
101219A	0.6 s	$4.6 \times 10^{-7}$ erg cm $^{-2}$	0.6	0.72

**Table 1.** Observed parameters of GRB 101219A. From left to right, the columns indicate: GRB identifier, burst duration, fluence in the 15–150 keV band, photon-number index  $\beta$  as a function of frequency  $dN/d\nu \propto \nu^{-\beta}$ , and the burst’s redshift. In Section 2.1, we use this particular GRB to show that a typical short GRB placed at 200 Mpc (LIGO volume) will be very bright. Consequently, the “off-axis” prompt emission could be detectable even for substantially misaligned observers. This increases the likelihood to detect these objects, using a LIGO trigger, even in the absence of a GRB trigger (data from Chornock & Berger 2011; Fong et al. 2015).

its efforts on studying off-axis afterglows from short GRBs, the “macronova/kilonova” and radio flare produced by the dynamical ejecta, and the emission from other components (e.g., the cocoon emission; Nakar & Piran 2017; Gottlieb, Nakar & Piran 2017). These signals are expected to peak  $\sim$  days to  $\sim$  years after the merger and are fainter compared to the prompt emission (e.g., Metzger & Berger 2012; Metzger 2017). Coupled with the fact that current GW detectors have very poor localization, associating these signals to a GW source will be difficult. This is where the “off-axis” prompt signal has a considerable advantage, since we expect to detect the prompt emission a few seconds after the GWs, we can capitalize on its temporal coincidence to make the detection. This will also make follow-up searches for the off-axis afterglow and macronova/kilonova easier. Hence, it is very likely that the first detected EM counterpart of a LIGO trigger involving a NS-NS merger will be the fainter, “off-axis” prompt emission from a short GRB jet.

### 3 NUMERICAL SIMULATIONS

We have recently run relativistic MHD simulations of AGN jets (Barniol Duran, Tchekhovskoy & Giannios 2017; hereafter BTG17) using the HARM code (Gammie, McKinney & Tóth 2003), with recent improvements (Tchekhovskoy, Narayan & McKinney 2011; Bromberg & Tchekhovskoy 2016). The initial conditions and numerical scheme of these simulations are adapted to the physical setup relevant to this work. We initiate the jets via the rotation of the central magnetized compact object. The jets are, therefore, launched magnetically dominated. By adjusting the density of the gas in the injection radius, the jet is launched with magnetization  $\mu = 2p_{\text{mag},0}/\rho_0 c^2 \simeq 25$ , where  $p_{\text{mag},0}$  is the magnetic pressure and  $\rho_0$  is the density at the base of the jet. The initial magnetization  $\mu$  determines maximum Lorentz factor of the jet. We do not take into account neutrino heating which may affect the structure of the jet (e.g., Barkov & Pozanenko 2011; Murguia-Berthier et al. 2017).

We considered a scenario in which a low-density funnel is carved along the z-axis at the start of the simulation and we have confined the jet to propagate along high-density walls (similar to “model B” simulations in BTG17). Our simulations, performed in both 2D and 3D, follow jets from the compact object to a scale  $\sim 10^3 \times$  larger. These large scale simulations allow us to follow the jet acceleration through conversion of its magnetic energy into kinetic energy. In the context of short GRB jets, as the jet breaks out from the confining medium, it essentially travels through vacuum (or at least very low ambient gas). This is quite advantageous since BTG17 have shown that these type of jets are almost identical

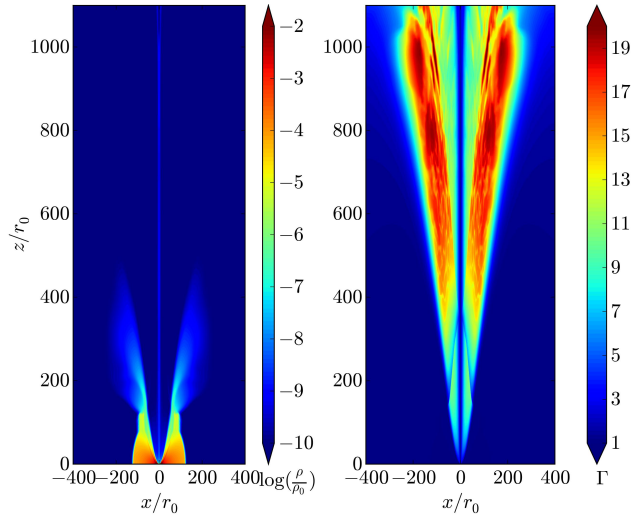


**Figure 2.** Numerical simulation of a jet that is collimated by and breaks out from the dynamical ejecta. We show 2D cuts of density (left panel) and Lorentz factor (right panel), where  $r_0$  stands for a few times the radius of the central compact object. The jet accelerates as it breaks out from the dynamical ejecta and spread sideways. At large distance the jet turns conical and its lateral structure is fixed.

in 2D and 3D runs and that they are fairly axisymmetric (see also Bromberg & Tchekhovskoy 2016). For this reason, we focus our efforts on axisymmetric 2D simulations, which are considerably less computationally expensive and can be better resolved numerically.

We mimicked the boundary of the dynamical ejecta by setting the ambient gas density of our previous simulations (see BTG17 model B-2D-vhr for details on jet and ambient gas parameters and numerical resolution) to be essentially zero beyond  $\sim 100$  times the size of the compact object as displayed in Fig. 2, which shows both density and velocity (Lorentz factor) contours. After the jet breaks out from the dynamical ejecta, a rarefaction wave crosses the jet and it spreads sideways and accelerates further (Tchekhovskoy, Narayan & McKinney 2010; Komissarov, Vlahakis & Königl 2010). For this work, we simulate “steady state” jets that will maintain the conditions at the central engine constant. This means that the rotation of the black hole and the magnetic field strength is kept constant, so that the jet has a constant power throughout the duration of the simulation. Future simulations will explore short-lived jets.

The distance where the radiation from the jet takes place is uncertain; the prompt emission may originate at the transparency radius of the jets or further out, at optically thin conditions (see next Section). The distance at which the jet produces the  $\gamma$ -ray radiation lies beyond our simulated region. However, we argue that the dynamical range of our current simulations is sufficient for the objectives of our estimates. This is due to the fact that after the phase of lateral expansion and the crossing of the rarefaction wave, the jet becomes approximately conical and its properties “freeze out” as a function of angle (see Fig. 3). Therefore, the lateral structure of the jet, which is the key aspect of our study, is set at this distance. It is no longer necessary to follow the jet beyond this point since its properties can be safely extrapolated at larger distances (Tchekhovskoy, Narayan & McKinney 2010). Our current simulations with a dynamical range of  $\sim 10^3$  already point towards this jet feature after breakout. Future simulations in 2D with even larger dynamical range will be able to test this effect in detail.

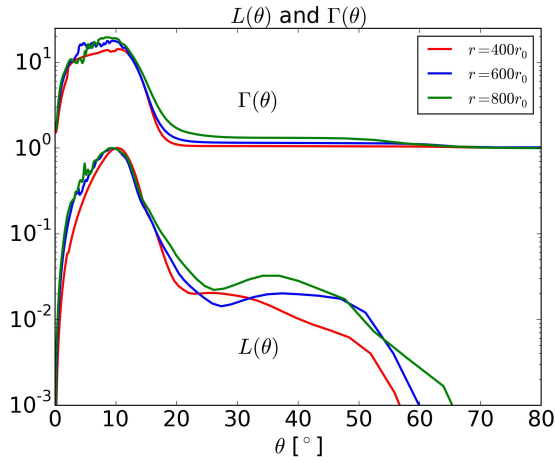


**Figure 3.** Jet luminosity,  $L(\theta)$  (arbitrary units), and jet Lorentz factor,  $\Gamma(\theta)$ , for different radii  $r$  from the compact object for our numerical simulation in Fig. 2.  $r_0$  stands for a few times the radius of the central compact object. The luminosity and Lorentz factor profiles are very similar for increasing radii, hence we can assume that the jet structure “freezes out” beyond a certain radius. This allows us to safely extrapolate the jet structure to even larger radii.

## 4 RESULTS AND DISCUSSION

We have extracted the jet luminosity  $L(\theta)$  and Lorentz factor  $\Gamma(\theta)$  from our simulation in Fig. 2 at different radii from the central object, see Fig. 3. The luminosity  $L(\theta)$  is the total (magnetic, kinetic and thermal) luminosity per solid angle of the jet  $L(\theta) = dL/d\Omega$ . We note that close to the jet axis ( $z$ -axis) the luminosity is very low and the velocity is quite small. The jet is characterized by a fast and luminous core of opening angle of  $\theta_j \sim 10^\circ$ . The typical cosmological GRB is observed through its core emission. However, for larger angles, the jet Lorentz factor and luminosity drop steeply but remain substantial. These features have been seen in MHD jets before (see, e.g., Tchekhovskoy, McKinney & Narayan 2008 and references therein), but the exact profiles of  $L(\theta)$  and  $\Gamma(\theta)$  should depend on their profiles right before breakout, which in turn depend on the properties of the dynamical ejecta (see Section 3). Future simulations will explore more realistic dynamical ejecta models (e.g., Hotokezaka et al. 2013; Nagakura et al. 2014). Recent hydrodynamical simulations also find an energetic component at large angles (e.g., Gottlieb, Nakar & Piran 2017), and this component is ascribed to the “inner” cocoon (shocked jet material). However in our simulations, the effect of the cocoon on the jet structure is minimized because we initiate our setup with an evacuated funnel, and the extended component (the “sheath”) we obtain consists of rarefied magnetized jet.

As seen in Fig. 3, far beyond the breakout radius, there is evidence that quantities “freeze out”, i.e., the jet shows a similar profile as a function of angle for increasing radii. We will make use of this fact and show how the observed luminosity can be extracted from our MHD simulations.

### 4.1 Calculating observed luminosity

We now briefly describe how to calculate the observed luminosity as a function of  $\theta_{\text{obs}}$  for a given  $L(\theta)$  and  $\Gamma(\theta)$ . All quantities in the local co-moving frame will be denoted with a prime and we employ spherical coordinates. Consider an infinitesimal patch of the jet located at a polar angle  $\theta$  from the jet axis and azimuthal angle of  $\varphi$

(where we take the observer to be located at  $\theta_{\text{obs}}$  and  $\varphi = 0$ , see Fig. 4). The portion of the jet within this patch moves with  $\Gamma(\theta)$  at an angle  $\alpha$  with respect to the line of sight of the observer, where  $\alpha$  is given by  $\cos \alpha = \cos \theta_{\text{obs}} \cos \theta + \sin \theta_{\text{obs}} \sin \theta \cos \varphi$ .

Suppose this patch subtends a solid angle  $d\Omega_p$  on the jet-surface, the luminosity through this patch will be  $L_p = L(\theta)d\Omega_p$ . Using a Lorentz transformation, the luminosity within this patch in the co-moving frame can be expressed as  $L'_p = L_p/\Gamma^2(\theta)$ . We assume a fixed fraction ( $\eta$ ) of this luminosity is converted into radiation. For simplicity, we further assume that the radiation is released instantaneously, is isotropic in the jet co-moving frame and is emitted at a fixed distance  $r_{\text{jet}}$ , which is justifiable since the jet structure “freezes out” at the distances we are considering, therefore the total luminosity from a gradual dissipation would give similar results. The radiated luminosity per unit solid angle in the co-moving frame is therefore  $\eta L'_p/4\pi$ . This luminosity per solid angle has to be boosted to the lab frame, taking into account the inclination  $\alpha$ . Therefore, each patch of the jet contributes

$$dL_{\text{obs}} = \Gamma(\theta)\delta^3 \frac{\eta L'_p}{4\pi} = \frac{\eta L(\theta)d\Omega_p}{4\pi\Gamma^4(\theta)[1 - \beta(\theta)\cos \alpha]^3}. \quad (1)$$

Finally, we add the contribution from all patches of the jet which amounts to an integral over the solid angle of the jet, hence,

$$L_{\text{obs}}(\theta_{\text{obs}}) = \int_0^{2\pi} \int_0^{\theta_e} dL_{\text{obs}}, \quad (2)$$

where  $\theta_e$  signifies the poloidal extent of the jet. This calculation shows that by extracting  $L(\theta)$  and  $\Gamma(\theta)$  from our simulations we can estimate the prompt emission seen by an observer at any angle. The observed luminosity of the core can be scaled to the observed average luminosity of on-axis short GRBs, which in turn can give us a count rate at a detector (e.g., *Fermi* or *Swift*). Fig. 4 shows the observed luminosity  $L_{\text{obs}}(\theta_{\text{obs}})$  (normalized to the peak luminosity) for our simulation in Fig. 2, using  $L(\theta)$  and  $\Gamma(\theta)$  shown in Fig. 3, taking  $\theta_e \sim 23^\circ$ , which marks the extent of the jet with substantial magnetization ( $\sigma \gtrsim 10^{-2}$ ). The observed luminosity decreases quickly as the angle from the jet axis increases; however, at large angles a significant contribution exists. In this example, the jet luminosity at  $\sim 40^\circ$  is a factor of  $\sim 300$  fainter than that of the jet core. Nevertheless, it is clear from the estimates presented in Section 2.1 that such a misaligned jet can be still detected, provided that it takes place within the Advanced LIGO detectability volume.

If we had considered the uniform core model for the jet with  $\Gamma_{\text{core}} \approx 20$ , the ratio of the observed luminosity at  $\theta_{\text{obs}} \approx 40^\circ$  to the on-axis ( $\theta \lesssim 10^\circ$ ) luminosity would be  $L(\theta_{\text{obs}})/L_{\text{core}} \simeq (\Gamma_{\text{core}}\theta_{\text{obs}})^{-6} \sim 10^{-7}$ , which would be negligible. Hence, the “off-axis” prompt emission from a structured jet is significantly larger than that from the uniform jet model, which greatly increases the prospects of detecting it.

The *steady jet* assumption considered above is valid as long as the GRB duration (defined for an on-axis observer) is  $T_{\text{GRB}} > r_{\text{jet}}/\Gamma^2 c$ , where  $r_{\text{jet}}$  is the radius at which the jet dissipation occurs, and the  $\gamma$ -rays for an on-axis observer are produced. If this condition is not satisfied then (i) the onset of the emission is delayed by  $\sim r_{\text{jet}}/\Gamma^2 c$  and (ii) the luminosity drops by a factor of  $\sim \Gamma^2 c T_{\text{GRB}}/r_{\text{jet}}$  with respect to the steady jet calculation performed above. This evidently depends on  $r_{\text{jet}}$  and  $\Gamma(\theta)$ , and therefore on a particular jet dissipation model. For an estimate, we will consider the *photospheric* model (e.g., Mészáros & Rees 2000; Giannios 2006) for the prompt GRB emission. This model predicts that the emission comes from the Thomson photosphere of the jet:  $r_{\text{jet}} = r_{\text{ph}} = L\sigma_T/4\pi\Gamma^2\mu m_p c^3$ . The corresponding delay of

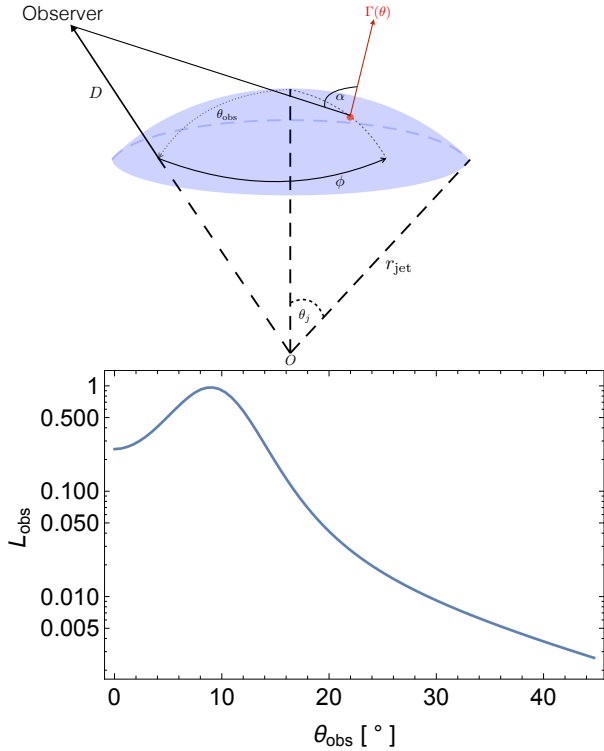


**Figure 4.** *Top panel:* Geometry of the conical jet, we use spherical coordinates with the origin at  $O$ . The observer is located at  $(D, \theta_{\text{obs}}, 0)$ . We consider a patch of this jet (red dot) at  $(r_{\text{jet}}, \theta, \varphi)$  moving with Lorentz factor  $\Gamma(\theta)$  with a corresponding angle  $\alpha$  between its velocity and line of sight of the observer. *Bottom panel:* Observed luminosity (normalized to peak) as a function of observer angle,  $L_{\text{obs}}(\theta_{\text{obs}})$ , for our jet simulation output presented in Fig. 3. The calculation was performed at  $r = 800r_0$ ,  $r_0$  is a few times the size of the compact object. In this example, the jet luminosity at  $\sim 40^\circ$  is a factor of 300 fainter than that of the jet core. Nevertheless, such a misaligned jet can be detected by a  $\gamma$ -ray instrument if it takes place within the Advanced LIGO detectability volume.

the prompt signal will be  $\sim r_{\text{jet}}/2\Gamma^2c \simeq L\sigma_T/8\pi\Gamma^4\mu m_p c^4 \sim 5L_{48}\Gamma_{0.5}^{-4}\mu_{1.5}^{-1}$  sec, where we use the notation  $A = 10^x A_x$  and  $cgs$  units. Here we see, that depending on the exact parameters, the signal from the sheath moving with  $\Gamma \sim 3$  and of luminosity  $L \sim 10^{48}$  erg-sec $^{-1}$  could be delayed by a few to few tens of seconds with respect to the GW signal.

## 5 CONCLUSIONS

In this work, we investigate a different electromagnetic counterpart of gravitational wave events, which is the “off-axis” prompt emission from the associated short GRB. We argue that in a realistically structured jet, the prompt emission can still be detected for substantially misaligned observers and we have performed simulations to support this claim. Even though this prompt signal is much fainter compared to an on-axis short GRB, we stress that the temporal coincidence with a LIGO trigger will be crucial in order to make it a significant detection. The localization of the “off-axis” prompt emission  $\gamma$ -rays will greatly facilitate the source localization, host galaxy identification and detection of longer wavelength signals expected days to years after the burst.

## ACKNOWLEDGMENTS

We thank Alexander Tchekhovskoy for useful discussions and the anonymous referee for valuable comments on the draft. We acknowledge support from NASA through the grants NNX16AB32G and NNX17AG21G issued through the Astrophysics Theory Program.

## REFERENCES

- Abbott B. P. et al., 2016a, *Physical Review Letters*, 116, 241103  
 Abbott B. P. et al., 2016b, *ApJ*, 826, L13  
 Abbott B. P. et al., 2016c, *Physical Review Letters*, 116, 241102  
 Abbott B. P. et al., 2016d, *Physical Review Letters*, 116, 221101  
 Barkov M. V., Pozanenko A. S., 2011, *MNRAS*, 417, 2161  
 Barniol Duran R., Tchekhovskoy A., Giannios D., 2017, *MNRAS*, 469, 4957  
 Berger E., 2014, *ARA&A*, 52, 43  
 Bromberg O., Tchekhovskoy A., 2016, *MNRAS*, 456, 1739  
 Chornock R., Berger E., 2011, *GRB Coordinates Network*, 11518  
 Connaughton V. et al., 2016, *ApJ*, 826, L6  
 Duffell P. C., Quataert E., MacFadyen A. I., 2015, *ApJ*, 813, 64  
 Eichler D., Livio M., Piran T., Schramm D. N., 1989, *Nature*, 340, 126  
 Fong W., Berger E., Margutti R., Zauderer B. A., 2015, *ApJ*, 815, 102  
 Gammie C. F., McKinney J. C., Tóth G., 2003, *ApJ*, 589, 444  
 Giannios D., 2006, *A&A*, 457, 763  
 Gottlieb O., Nakar E., Piran T., 2017, *ArXiv e-prints*  
 Hotokezaka K., Kiuchi K., Kyutoku K., Okawa H., Sekiguchi Y.-i., Shibata M., Taniguchi K., 2013, *Phys. Rev. D*, 87, 024001  
 Hotokezaka K., Piran T., 2015, *MNRAS*, 450, 1430  
 Kasen D., Badnell N. R., Barnes J., 2013, *ApJ*, 774, 25  
 Kochanek C. S., Piran T., 1993, *ApJ*, 417, L17  
 Komisarov S. S., Vlahakis N., Königl A., 2010, *MNRAS*, 407, 17  
 Lamb G. P., Kobayashi S., 2017, *ArXiv e-prints*  
 Lazzati D., Deich A., Morsony B. J., Workman J. C., 2017, *MNRAS*, 471, 1652  
 Lee W. H., Ramirez-Ruiz E., 2007, *New Journal of Physics*, 9, 17  
 Li L.-X., Paczyński B., 1998, *ApJ*, 507, L59  
 Martynov D. V. et al., 2016, *Phys. Rev. D*, 93, 112004  
 Mészáros P., Rees M. J., 2000, *ApJ*, 530, 292  
 Metzger B. D., 2017, *Living Reviews in Relativity*, 20, 3  
 Metzger B. D., Berger E., 2012, *ApJ*, 746, 48  
 Metzger B. D. et al., 2010, *MNRAS*, 406, 2650  
 Murguia-Berthier A., Montes G., Ramirez-Ruiz E., De Colle F., Lee W. H., 2014, *ApJ*, 788, L8  
 Murguia-Berthier A. et al., 2017, *ApJ*, 835, L34  
 Nagakura H., Hotokezaka K., Sekiguchi Y., Shibata M., Ioka K., 2014, *ApJ*, 784, L28  
 Nakar E., 2007, *Phys. Rep.*, 442, 166  
 Nakar E., Piran T., 2011, *Nature*, 478, 82  
 Nakar E., Piran T., 2017, *ApJ*, 834, 28  
 Patricelli B., Razzano M., Cella G., Fidecaro F., Pian E., Branchesi M., Stamerra A., 2016, *JCAP*, 11, 056  
 Pescalli A., Ghirlanda G., Salafia O. S., Ghisellini G., Nappo F., Salvaterra R., 2015, *MNRAS*, 447, 1911  
 Rezzolla L., Giacomazzo B., Baiotti L., Granot J., Kouveliotou C., Aloy M. A., 2011, *ApJ*, 732, L6  
 Rossi E., Lazzati D., Rees M. J., 2002, *MNRAS*, 332, 945

- Rosswog S., 2013, *Philosophical Transactions of the Royal Society of London Series A*, 371, 20120272
- Salafia O. S., Ghisellini G., Pescalli A., Ghirlanda G., Nappo F., 2015, *MNRAS*, 450, 3549
- Sapountzis K., Vlahakis N., 2014, *Physics of Plasmas*, 21, 072124
- Tchekhovskoy A., McKinney J. C., Narayan R., 2008, *MNRAS*, 388, 551
- Tchekhovskoy A., Narayan R., McKinney J. C., 2010, *New Astronomy*, 15, 749
- Tchekhovskoy A., Narayan R., McKinney J. C., 2011, *MNRAS*, 418, L79
- Wanderman D., Piran T., 2015, *MNRAS*, 448, 3026